Journal of Controlled Release 259 (2017) 203–211

Contents lists available at ScienceDirect

Journal of Controlled Release

journal homepage: www.elsevier.com/locate/jconrel

Andrographolide-loaded polymerized phenylboronic acid nanoconstruct for stimuli-responsive chemotherapy

Jinhwan Kim [a,1], Junseok Lee [b,1], Yeong Mi Lee [b], Swapan Pramanick [a], Sooseok Im [c], Won Jong Kim [a,b,c,*]

[a] Department of Chemistry, Pohang University of Science and Technology (POSTECH), Pohang 37673, Republic of Korea
[b] Center for Self-assembly and Complexity, Institute of Basic Science (IBS), Pohang 37673, Republic of Korea
[c] School of Interdisciplinary Bioscience and Bioengineering, Pohang University of Science and Technology (POSTECH), Pohang 37673, Republic of Korea

ARTICLE INFO

Article history:
Received 14 August 2016
Received in revised form 5 October 2016
Accepted 26 October 2016
Available online 28 October 2016

Keywords:
Andrographolide
Phenylboronic acid
Boronic ester chemistry
Drug delivery
Tumor targeting

ABSTRACT

Along with the successful discovery of paclitaxel as an anticancer drug, natural products have drawn great attention in drug discovery. Recently, andrographolide (AND) from *Andrographis paniculata* was reported to provide several benefits, including an anticancer effect. However, the extremely low solubility of the compound in an aqueous medium was an obstacle to overcome for the systemic administration and clinical application of AND. Based on our previous report, we formulated a water-soluble nanoconstruct by forming a boronic ester between the *cis*-1,3-diol of AND with hydrophilically polymerized phenylboronic acid (pPBA). The release of loaded AND was controlled by intracellular conditions, specifically, by low pH and high ATP concentrations, due to the pH- and diol-dependent affinity of the boronic ester. Because of the intrinsic property of the PBA moiety, the pPBA-AND nanoconstruct exhibited an excellent tumor targeting ability both *in vitro* and *in vivo*. Finally, a significant inhibition of tumor growth was observed *in vivo*. Taken together, our strategy, which is based on the formulation of a soluble nanoconstruct using hydrophilically polymerized PBA and a *cis*-diol, is plausible and provides a delivery system for a wide variety of chemotherapeutics. This strategy has applications not only in cancer therapy but also broader fields such as anti-inflammation or immunotherapy.

1. Introduction

For several decades, secondary metabolites derived from natural organisms such as plants or microbes have been regarded as "natural products", and they have attracted an enormous interest for various clinical applications [1–3]. To date, many kinds of natural products have been discovered and their biological activities have been evaluated [4,5]. In particular, paclitaxel from the pacific yew, salicylic acid from willow, and penicillin G from *Penicillium citrinum* are good examples of successfully commercialized natural products. Recently, an active compound called andrographolide (AND) was discovered from the extract of *Andrographis paniculata*, an herbaceous plant known as "king of bitter" [6,7]. Several studies have found that AND, along with its derivatives, modulates cellular signaling pathways. Moreover, they exhibit various beneficial effects such as antioxidant defense, anti-inflammatory effect, immunomodulatory activity, hepatoprotective activity, antiviral effect, and anticancer effect [8–11]. Especially, many reports have demonstrated that anticancer activity of AND is exerted by affecting various cancer-related factors, thus inhibits the proliferation, metastasis, and angiogenesis of cancer cells. In spite of these studies suggesting AND as a promising candidate for anticancer chemotherapeutics, an *in vivo* evaluation of its effect as an anticancer drug has been barely reported due to the extremely low solubility of AND in an aqueous medium [12]. Similar to other hydrophobic anticancer drugs, including paclitaxel and camptothecin, addition of a surfactant or organic solvent such as dimethyl sulfoxide (DMSO) or alcohol could be an alternative to solubilize AND in an aqueous medium [13–15]. However, these solubilizing agents may induce acute hemolysis leading to fatal systemic damage; additionally, the concern of cryptotoxicity still exists [16–18].

In drug delivery system, a nano-sized formulation has been widely attempted because it enables tumor-specific extravasation *via* an enhanced permeation and retention (EPR) effect [19–26]. Thus far, various types of nano-sized delivery systems, including liposomes, polymeric micelles, and inorganic nanoparticles, have been employed [27–31]; of these, liposomes, polymeric micelles, and self-assembled conjugates are the most commonly applied strategies. However, liposomes and polymeric micelles lack *in vivo* stability after administration, leading to nonspecific leakage of the loaded drug [32,33]. In addition, self-assembled conjugates require the chemical modification of drug molecules, which may reduce their therapeutic effect; they also require complicated synthetic procedures, which may hinder highly reproducible results [21,32,33]. Remarkably, the chemical structure of AND suggests an

* Corresponding author at: Department of Chemistry, Pohang University of Science and Technology (POSTECH), Pohang 37673, Republic of Korea.
E-mail address: wjkim@postech.ac.kr (W.J. Kim).
[1] These Authors are contributed equally to this work.

http://dx.doi.org/10.1016/j.jconrel.2016.10.029
0168-3659/

ingenious solution for a delivery system that overcomes aforementioned challenges for a drug delivery carrier when combined with hydrophilic polymers and phenylboronic acid (PBA). It has been widely known that PBA, (chemical formula: $C_6H_5B(OH)_2$), has a unique ability to form a boronic ester bond with a *cis*-1,2- or -1,3-diol, a common moieties of saccharides; thus, it has been incorporated as a ligand in applications for sugar sensors or affinity column of carbohydrates [34–37]. Specifically, PBA seems like a highly appropriate chemical moiety for delivery applications for two reasons. First, the binding affinity of PBA and diol is highly sensitive to external conditions including pH, sugars, and H_2O_2, making PBA moieties the preferred choice in stimuli-responsive drug delivery systems [38–41]. Second, PBA itself can act as a cancer targeting ligand because it exhibits specific binding with sialylated epitopes that are overexpressed on the surface of various types of tumors [42–44]. Using these characteristics, our group has reported a stimuli-responsive cross-linked polyethyleneimine for effective gene delivery based on the interaction between PBA and galactose [45]. Similarly, in the case of AND, which has 5-hydroxymethyl and 6-hydroxyl groups in the *cis* position to form a 1,3-*cis*-diol, it is expected that AND and PBA would form a boronic ester bond, subsequently generating their hydrophobic chemical structure. PBA is conjugated on a hydrophilic polymer; therefore, it is obvious that a self-assembled structure would be formed from the hydrophilic polymer backbone and the hydrophobic PBA-AND complex. The fact that they form a self-assembled structure could provide a great opportunity to expand the accessibility of AND to a drug delivery system.

By employing particular properties of PBA and AND in biomedical applications, we developed a simple and unique polymeric platform for the systemic administration of AND to be used as effective chemotherapy by overcoming limitations of aforementioned previous studies (Scheme 1). The PBA moiety was grafted on poly(methyl vinyl ether *alt* maleic anhydride) (pMAnh) to form poly(phenylboronic acid) (pPBA). It is worth highlighting that the synthetic procedure of pPBA does not require the usage of neither toxic solvents nor catalysts, thus it is free from residual solvent toxicity; additionally, it is highly atom economical and favors green chemistry. Next, a nanoconstruct was formulated by simple mixing pPBA and AND at the desired molar ratio. The pPBA-AND nanoconstruct was preferred because of several advantages: 1) it did not require any complicated synthetic procedure; 2) large amounts of carboxylic acid (derived from hydrolyzed pMAnh) readily solubilized and stabilized AND in an aqueous medium; 3) the residual PBA moiety exhibited a tumor targeting effect; 4) the hydrodynamic size of ~100 nm was suitable for biomedical applications; and 5) loaded AND was released specifically intracellularly. This unique strategy could provide an innovative platform for the delivery of hydrophobic AND and its derivatives, not only for cancer therapy, but also for more broad applications such as anti-inflammatory therapy or immunotherapy.

2. Materials and methods

2.1. Materials

Poly(methyl vinyl ether-*alt*-maleic anhydride) (pMAnh; Mn ~80,000), 3-aminophenylboronic acid monohydrate (PBA-NH_2), adenosine 5′-triphosphate disodium salt hydrate (ATP), thiazolyl blue tetrazolium bromide (MTT) and all other solvents were purchased from Sigma Aldrich Co. (St. Louis, MO). Flamma FCR648-NH_2 was purchased from BioActs (Incheon, Korea). All reagents were used as received without further purification.

2.2. Instrumental methods

TEM image was taken from a transmission electron microscope (JEM-2210, JEOL) and analyzed by Gatan DigitalMicrograph software. UV–vis spectra were measured from a UV–vis spectrometer (UV 2550, Shimadzu) and fluorescence spectra were measured from a spectrofluorophotometer (RF-5301 PC, Shimadzu). Hydrodynamic volume and zeta potential were measured from zetasizer (Nano S90, Nano Z, respectively; Malvern) at 0.1 mM in Dulbecco's phosphate buffered saline (DPBS, pH 7.4) or PBS (pH 5.0). Confocal laser scanning microscope (CLSM) image was obtained from Olympus FV-1000 and analyzed by OLYMPUS FLUOVIEW ver. 1.7a Viewer software.

2.3. Extraction of andrographolide (AND) from A. paniculata

The air-dried powdered leaves of *Andrographis paniculata* (1 kg) were subjected to extraction in a Soxhlet apparatus with light petroleum ether (bp 60–80 °C), $CHCl_3$, and MeOH respectively. The MeOH extract was partitioned between *n*-BuOH and water. The *n*-BuOH extract (15 g), obtained after evaporation of solvent *in vacuo*, was

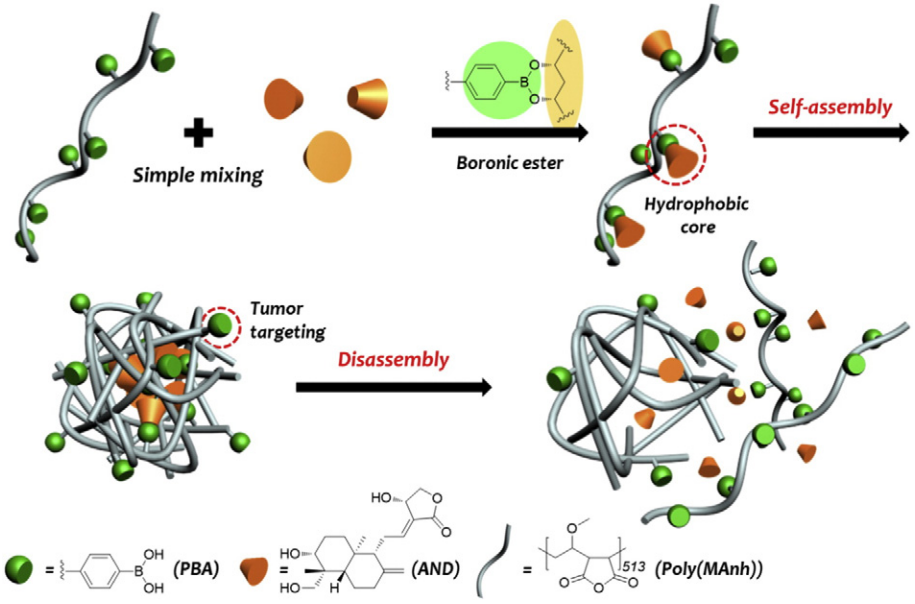

Scheme 1. Schematic illustration for the formulation and destruction of the pPBA-AND nanoconstruct. The nanoconstruct is formulated by the interaction between PBA (from pPBA) and 1,3-*cis*-diol (from AND), followed by self-assembly based on the hydrophobic interactions of AND and PBA. Furthermore, the nanoconstruct is disassembled, leading to the release of AND, in response to an intracellular stimulus such as acidic pH or increased level of ATP.

chromatographed on a column of silica gel (mesh 60–120) with gradient elution starting from chloroform followed by various mixtures of $CHCl_3$ and MeOH. A fraction eluted with 12% methanolic chloroform yielded a compound (2.5 g), crystallized from methanol as colorless plates, m. p. 230–231 °C; $[\alpha]^{25}_D$ −112.7° (c 0.53, MeOH). The structure of the compound was established by detailed spectral studies (IR, ^{1}H & ^{13}C NMR, and ESI-MS, supporting information). Finally, the compound was identified as andrographolide by direct comparison with an authentic sample.

2.4. Preparation of poly{[methyl vinyl ether-alt-maleic acid]-co-[methyl vinyl ether-alt-(N-3-boronophenyl-maleamic acid)]} (pPBA)

PBA-conjugated pMAnh was prepared by ring opening reaction between succinic anhydride moiety of pMAnh and amine-functionalized PBA-NH_2 (Scheme S1). Briefly, 500 mg of pMAnh (3.2 mmol succinic anhydride equivalence) was dissolved in 10 mL of dry DMSO. PBA-NH_2 (160 mg, 1 mmol) was added into the solution and stirred at RT for 24 h. NaOH (0.1 N, 10 mL) was added to hydrolyze the residual succinic anhydride moiety and dialyzed against DW for 2 days (MWCO = 10,000). The final product was obtained by lyophilization. Conjugation ratio of PBA was calculated by ^{1}H NMR. (Yield: 91%)

^{1}H NMR (D_2O, 300 MHz): 7.7–7.0 (m, Ph, 4xH); 3.8–3.5 (m, -CH-, 1H); 3.5–3.1 (m, -OCH_3, 3H); 3.1–2.4 (m, CHCOO, 2H); 2.4–1.4 (m, -CH_2-, 2H).

In addition, FCR648-NH_2 was co-conjugated on the pMAnh backbone to introduce the fluorescence moiety for bio-imaging. Briefly, 200 mg of pMAnh was dissolved in 10 mL of dry DMSO. PBA-NH_2 (70 mg) and FCR648-NH_2 (5 mg) were added into the solution and stirred at RT for 24 h. NaOH (0.1 N, 1 mL) was added dialyzed for 2 days (MWCO = 10,000). The final product was obtained by lyophilization. Conjugation ratio of PBA was calculated by ^{1}H NMR. (Yield: 95%).

2.5. Formulation of pPBA-AND nanoconstruct (pPBA-AND-11 and pPBA-AND-21)

pPBA-AND nanoconstruct was formulated by simple mixing method. For the formulation of nanoconstruct of 1:1 M ratio (pPBA:AND) with final concentration of 5 mM AND, 100 μL of 50 mM pPBA was added into the 20 μL of 250 mM AND in DMSO (pPBA-AND-11). The solution was mixed thoroughly and filled up to 1 mL by DPBS to obtain pPBA-AND-11 solution. For 2:1 ratio (pPBA-AND-21), 100 mM pPBA rather than 50 mM pPBA was utilized in a same manner.

2.6. pH-responsive affinity between PBA and diol

A pH-responsive binding between PBA and diol was measured by monitoring the quenching of intrinsic fluorescence from PBA moiety. In brief, 0.1 mM pPBA containing 20, 10, 5, 0.5 or 0 mM AND were prepared in DPBS (pH 7.4) or PBS (pH 5.0). The fluorescence intensity of PBA moiety (ex = 302 nm and em = 388 nm) was measured and plotted with Stern-Volmer equation.

2.7. Investigation of drug release profile

The *in vitro* release of AND was examined using dialysis bag (MWCO = 3500) depending on different incubation time within a water-soluble range [12]. Briefly, free AND, pPBA-AND-11, and pPBA-AND-21 those containing 1 mM AND respectively were loaded in a dialysis bag. Samples were dialyzed against 50 mL of DPBS buffer (pH 7.4) or PBS (pH 5.0), and DPBS containing 5 mM ATP. At each time point, 200 μL of dialyzing buffer was transferred, and the absorbance at 265 nm was detected in order to measure the release of AND. The release of free AND for 48 h incubation was designated as 100% AND release.

2.8. Cell viability test in vitro

Cytotoxicity of the materials was evaluated under various concentrations. Cells (MCF-7 and PC-3) were seeded on 96 well culture plate at a density of 8000 cells/well and incubated for overnight. A solution of pPBA, AND, pPBA-AND-11 and pPBA-AND-21 at final concentration of 0 to 100 μM was treated with fresh medium and incubated for further 48 h. After incubation, cell viability was evaluated by MTT assay.

For MTT assay, cells were washed with DPBS and the medium was replaced by 200 μL of MTT solution in medium (0.5 mg/mL). After incubation at dark for 4 h, medium was removed thoroughly and purple crystal was completely dissolved by 200 μL of DMSO. 100 μL of each sample was transferred into a new 96 well plate and UV–vis absorbance at 570 nm was measured by a microplate spectrofluorometer (VICTOR3 V multilabel counter). The relative percentages of non-treated cells were used to represent 100% of cell viability.

2.9. Competition assay in vitro

For the competition assay, cells (MCF-7 and PC-3) were prepared as the same way in cell viability test *in vitro*. Before treatment of sample, cells were pre-incubated with free PBA (5 mM) for 30 min. In the media containing 5 mM free PBA, free AND and pPBA-AND-21 at final concentration of 0 to 100 μM was treated and further incubated for 48 h. Cell viability was measured using MTT assay which is explained in upper section.

2.10. Intracellular uptake of nanoconstruct monitored by confocal laser scanning microscopy (CLSM) image

The MCF-7 cells were seeded on 12-well plates over glass coverslips at an initial density of 20,000 cells/well and incubated overnight in 5% CO_2 humidified incubator. FCR-pPBA-AND nanoconstructs [11 and 21] containing 10 μM AND were treated and incubated for 6 h with and without the pre-incubation with 5 mM free PBA. In case of pPBA-AND-21, same molar ratio of pPBA and FCR-pPBA were mixed in order to normalize the fluorescence signal with FCR-648 labelled pPBA-AND-11. After quenching the cellular uptake by adding cold DPBS, cells were washed and fixed with 10% neutral buffered formalin (NBF) solution for overnight. Cells on coverslips were mounted in mounting medium containing DAPI and observed with CLSM. Images were obtained and analyzed with Olympus Fluoview ver. 1.7a viewer software.

2.11. Flow cytometry

The MCF-7 cells were seeded on 6-well plates at an initial density of 200,000 cells/well and incubated overnight in 5% CO_2 humidified incubator. FCR-pPBA, FCR-pPBA-AND-11 FCR-pPBA-AND-21 (containing 10 μM AND) were treated and incubated for 6 h with and without the pre-incubation with 5 mM free PBA. Same as CLSM imaging, pPBA-AND-21 was formulated with FCR-pPBA and pPBA to normalize the signal intensity with pPBA-AND-11. After incubation, cold DPBS was added to stop the cellular uptake and washed with DPBS several times to remove nonspecific binding. The cells were then harvested by trypsinization, and resuspended in DPBS. The flow cytometry data of the cells were analyzed with a FACS Calibur (Becton Dickinson) and BD Cell Quest software (Becton Dickinson), by following the manual provided from the manufacturer.

2.12. Hemolysis assay

Hemolysis induced by each sample was evaluated by measuring the release of hemoglobin from the erythrocytes. In brief, fresh mouse blood was diluted 10 folds in PBS, and subsequently centrifuged at 2000 rpm for 15 min. Samples containing 0.5 mM AND

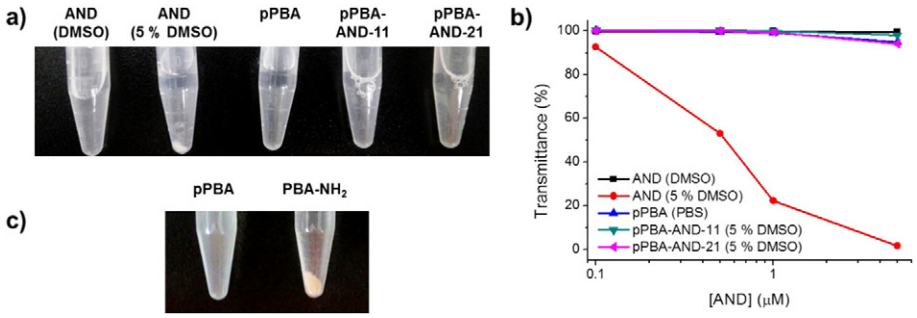

Fig. 1. Solubility profiles of each formulation. a) Solution of 5 mM AND in DMSO, AND in 5% DMSO, pPBA in PBS, pPBA-AND-11 and pPBA-AND-21 in 5% DMSO and b) corresponding transmittance of each solution measured at 500 nm. c) Solution of pPBA and PBA-NH_2 (100 mM) in PBS.

(free AND in 10% DMSO, pPBA, pPBA-AND-11, and pPBA-AND-21) were added in the diluted blood cells, and the resulting suspensions were incubated at 37 °C for 6 h. After incubation, suspensions were centrifuged at 2000 rpm for 15 min to make erythrocytes pellet. The absorbance of supernatants was measured at 541 nm in order to calculate the hemoglobin release. Saline and 1× lysis buffer were utilized as negative control (0% hemolysis) and positive control (100% hemolysis), respectively.

2.13. Biodistribution of pPBA-AND nanoconstruct in vivo

All animal experiments were approved by the POSTECH Biotech Center Ethics Committee. MCF-7 cells were inoculated subcutaneously (*s.c.*) at an initial density of 5×10^7 cells/mouse into the flank of female Balb/c-nu/nu mice. After the average tumor volume reached 300 mm^3, FCR-pPBA, FCR-pPBA-AND-11, and FCR-pPBA-AND-21 (15 mg/kg AND) were injected intravenously (i.v.). The 2:1 nanoconstruct was formulated with same molar ratio of FCR-pPBA and pPBA to normalize fluorescence signal as described in CLSM and flow cytometry analysis. At 24 h post i.v. injection, the mice were sacrificed and the fluorescence intensity of each organ was measured with an IVIS spectrum small-animal *in vivo* imaging system at Pohang Technopark Biotech Center (Califer Lifescience, Hopkinton, MA).

2.14. Monitoring tumor growth of mice

MCF-7 cells were inoculated *s.c.* at an initial density of 5×10^7 cells/mouse into the flank of each female Balb/c-nu/nu mice. When the average tumor volume was 100 mm^3, the mice were divided randomly into 5 groups (5 mice per group). The mice were then injected with 200 μL of each sample: 1) saline, 2) pPBA, 3) free AND containing 10% DMSO to solubilize AND, 4) pPBA-AND-11 and 5) pPBA-AND-21 (30 mg/kg AND), and the tumor volume was monitored every otherday after systemic injection of samples. Tumor volumes were recorded following the equation for a prolate ellipsoid: [tumor volume = $(ab^2/2)$], where a is the longest and b is the shortest dimension. The tumor growth was monitored when the tumor was ulcerated, at which time the mice were sacrificed according to the POSTECH Biotech Center Ethics Committee. All data was represented as mean ± SE and all statistical differences were analyzed using the software GraphPad Prism 6.

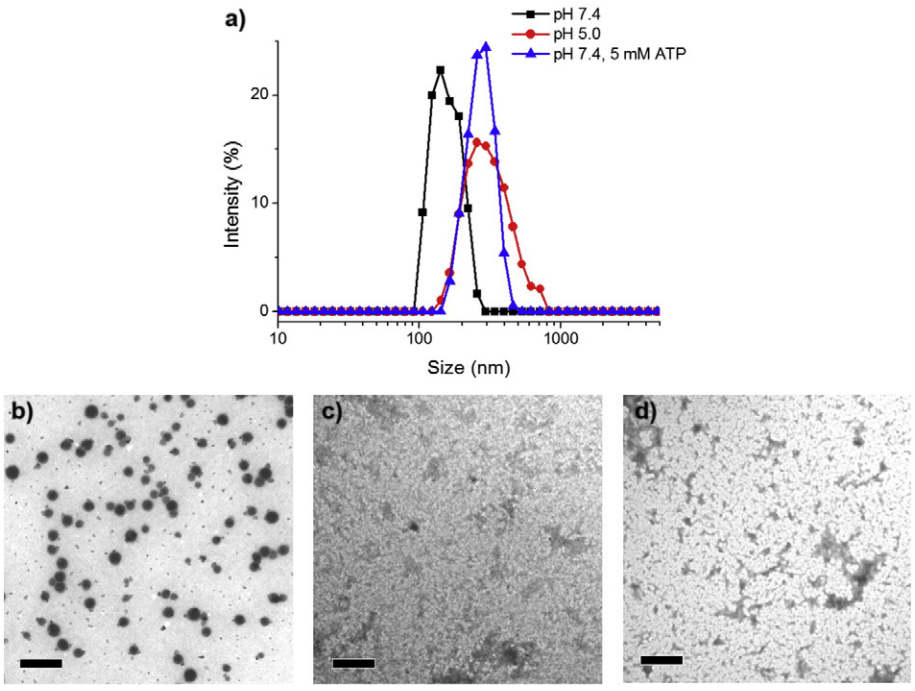

Fig. 2. Characterization of pPBA-AND nanoconstruct. a) Hydrodynamic size distribution of pPBA-AND-21 in different pH- and ATP-conditions and corresponding TEM images at b) pH 7.4, c) pH 5.0, and d) pH 7.4 with 5 mM ATP. Scale bar is 0.5 μm.

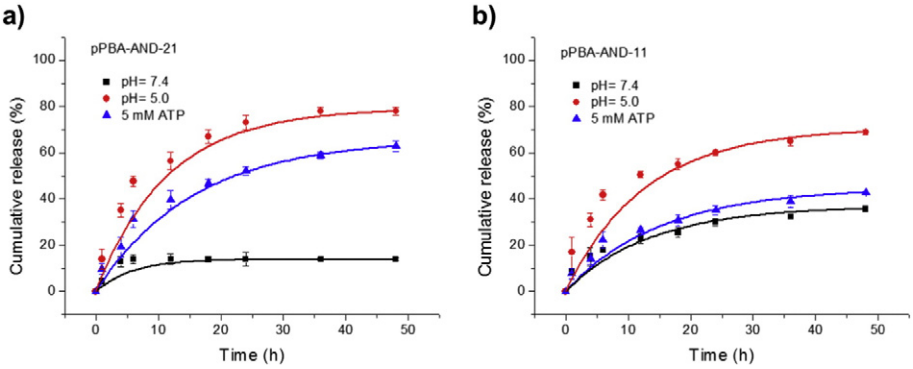

Fig. 3. Stimuli-responsive drug release of a) pPBA-AND-21 and b) pPBA-AND-11 under intracellular pH and ATP concentrations.

3. Results and discussion

3.1. Preparation and characterization of pPBA-AND nanoconstructs

In order to solubilize AND into an aqueous solution, pPBA was synthesized by a ring-opening reaction between the succinic anhydride moiety on pMAnh and amine-functionalized PBA (PBA-NH_2). Although there is a previously reported synthetic method for the preparation of pPBA [46], it requires a toxic organic solvent and thermal activation up to 90 °C, thus impeding the introduction of fluorescence dyes or thermo-sensitive biological molecules. On the other hand, in this report, a simple mixing of pMAnh and PBA-NH_2 in DMSO at room temperature with a subsequent hydrolysis step produced the PBA pendant-modified hydrophilic polymer, pPBA (Scheme S1). It is worth highlighting that this reaction was performed at room temperature and did not require any toxic organic solvent or additional catalyst; thus, 1) it is highly atom economical and 2) any amine-modified functional molecules can be easily introduced [21]. In this regard, an amine-functionalized fluorescent dye (FCR648-NH_2) was conjugated to pPBA to obtain the dye-labelled pPBA (FCR-pPBA). The molar ratio of PBA on pPBA was calculated as 156 PBA moieties per 513 repeating units using ^{1}H NMR (Fig. S1). In addition, a peak change of the C═O stretch from anhydride (1830–1800 cm^{-1} and 1775–1740 cm^{-1}, pMAnh) to carboxylic acid (1730–1700 cm^{-1}, maleic acid unit) and amide (1680–1630 cm^{-1}, PBA-conjugated maleamic acid unit) indicated the successful introduction of PBA on the pMAnh backbone (Fig. S2).

As mentioned above, the extremely low solubility of AND in an aqueous solution hinders the biomedical application of this compound as an anticancer or immunotherapy [12]. In order to surpass such drawbacks and apply the drug in a suitable delivery system, a pPBA-AND nanoconstruct was formulated by simple mixing of pPBA and an AND solution at the desired PBA:AND molar ratio of 1:1 and 2:1 (pPBA-AND-11 and pPBA-AND-21 respectively). As expected, 5 mM AND was well solubilized in DMSO, whereas it was readily precipitated by addition of an aqueous buffer at a final concentration of 5% DMSO/PBS, which was further represented by low transmittance (Fig. 1a–b). Otherwise, AND was solubilized into an aqueous medium (5% DMSO/PBS) upon addition of pPBA; both 1:1 and 2:1 nanoconstructs were well dispersed in an aqueous solution. Moreover, grafting PBA onto pMAnh also increased the solubility of PBA up to 100 mM (Fig. 1c); this is possibly due to the introduction of a carboxylic group on the polymer backbone. The content of AND in pPBA-AND-11 and pPBA-AND-21 was 34% and 20% (w/w) respectively.

3.2. Stimuli-responsive behaviors of pPBA-AND nanoconstructs

It is widely known that formation of a boronic ester between PBA and *cis*-diol is highly responsive to external conditions such as acidic pH or other diols (Scheme S2) [38–44]. Because quenching of the intrinsic fluorescence of PBA is induced through interaction with a diol, a pH- and concentration-dependent quenching was measured and plotted using the Stern-Volmer equation (Fig. S3) [42,45]. As demonstrated in Fig. S3b, a steady-state quenching of PBA was observed with increasing concentrations of AND, indicating the high affinity of AND and PBA in comparison with other sugar moieties [45]. Moreover, a lower slope at acidic conditions represented a pH-responsive affinity difference.

In this study, pPBA was designed to solubilize AND *via* formation of a nanoconstruct based on the interaction between the PBA moiety and a diol of AND. Owing to the environment-specific binding affinity of the boronic ester, both intracellular endosomal acidic pH (~5.0) and high concentrations of ATP ([ATP], 5–10 mM) were expected to influence the pPBA-AND nanoconstruct. In this regard, both pH- and [ATP]-responsive properties of pPBA materials were evaluated by monitoring its size distribution at pH 7.4, pH 5.0, or 5 mM ATP using dynamic light scattering (DLS). In the case of pPBA, size was slightly decreased at pH 5.0 due to more hydrophobic characteristics of the carboxylic group (protonation at lower pH), while no significant differences were induced by addition of ATP (Fig. S4b). The size distribution of pPBA-

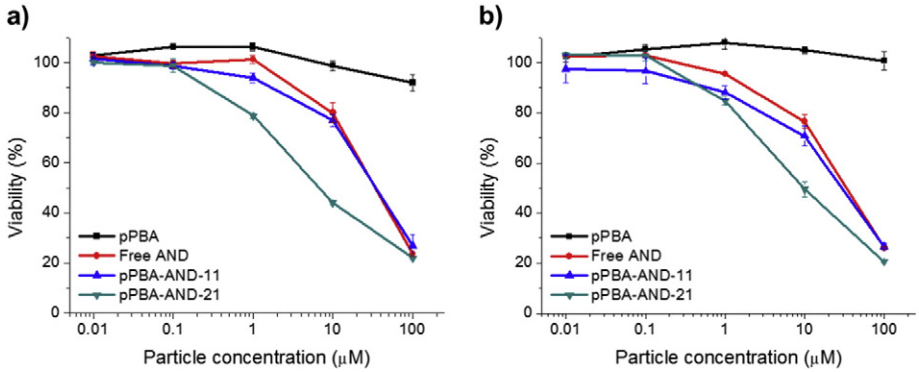

Fig. 4. Dose-dependent cytotoxicity of pPBA, AND, pPBA-AND-11, and pPBA-AND-21 against a) MCF-7 and b) PC-3 cell lines after 48 h incubation.

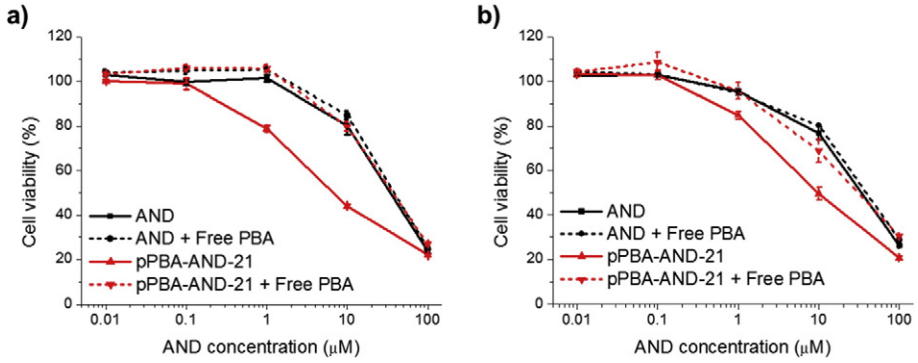

Fig. 5. *In vitro* competition assay. Cytotoxicity of AND and pPBA-AND-21 against a) MCF-7 and b) PC-3 cell lines after 48 h incubation with or without pre-treatment of free PBA (5 mM).

AND-11 was broadened at acidic pH and AND was readily precipitated at 5 mM ATP, resulting in the loss of signal in DLS (Fig. S4). Interestingly, pPBA-AND-21 showed the smallest size at pH 7.4 indicating a strong boronic ester and hydrophobic interaction, which was also observed by TEM images (Fig. 2a–b). On the other hand, the size distribution of pPBA-AND-21 was dramatically changed at both acidic pH and high [ATP]. Under these conditions, we could no longer observe an apparent structure from TEM images, which reveals the destruction of the nanoconstruct and successful release of AND (Fig. 2a, c–d).

In order to prove the stimuli-responsive release of AND, the release profile of AND from pPBA-AND nanoconstructs was evaluated at different pH and [ATP] (Fig. 3). The result in Fig. 3a demonstrates that approximately 80% and 60% of AND was released from pPBA-AND-21 after 48 h at intracellular pH and in the presence of ATP, respectively. However, at neutral pH without ATP, negligible amounts of AND were released, suggesting the pH and ATP dual-sensitive AND release from the 2:1 nanoconstruct. AND release from pPBA-AND-11 was also regulated by acidic pH and [ATP]; however, the sensitivity to each stimulus was lower than that of the 2:1 nanoconstruct, which might be due to the relatively low stability of the 1:1 nanoconstruct (Fig. 3b).

3.3. In vitro anticancer effect and tumor targeting

Favorable properties of pPBA-AND nanoconstruct, such as high drug contents (around 20% w/w for pPBA-AND-21), suitable size (~100 nm), and intracellular pH-responsive drug release, strongly suggest the therapeutic potential of the pPBA-AND nanoconstruct; moreover, a cancer-targeting effect of the residual PBA moiety is expected. In order to demonstrate the therapeutic effect of the nanoconstruct, the *in vitro* cytotoxicity of AND and pPBA-AND nanoconstructs was evaluated (Fig. 4). Owing to the strong negative charge and biocompatibility of hydrolyzed pMAnh, pPBA did not show any significant cytotoxicity as we reported previously [21]. Free AND exhibited an IC_{50} value of around 30 μM, which is similar to that of pPBA-AND-11. Interestingly, the IC_{50} value of pPBA-AND-21 was 5.1- or 3.5-fold lower than that of free AND in a MCF-7 or PC-3 cell line, respectively, which might be due to the targeting ability of residual PBA moieties.

In order to demonstrate the targeting ability of residual PBA, free PBA was pre-treated before treatment of pPBA-AND nanoconstructs to conduct the competition assay (Fig. 5). Pre-treated 5 mM PBA was expected to bind with sialylated epitopes on the cellular membrane and occupy the binding domain of cancer cells, thus inhibiting the cellular uptake of our nanoconstructs [42,45]. As shown in Fig. 5, the cytotoxicity of AND was maintained regardless of pre-treatment of free PBA, whereas that of pPBA-AND-21 was decreased dramatically to a level similar of free AND (in the case of pre-treatment of free PBA). This result implies the targeting ability of residual PBA of pPBA-AND-21.

To further confirm the residual PBA-assisted targeting effect in a quantitative manner, flow cytometry was performed with the nanoconstruct formulated by fluorescent dye labelled pPBA (FCR-pPBA). As shown in Fig. 6a, pPBA-AND-21 exhibited 2-fold higher cellular internalization in comparison to pPBA-AND-11, in accordance with the confocal microscopic image presented in Fig. 6b, where it is observed a stronger fluorescence signal from the 2:1 nanoconstruct compared with the 1:1 nanoconstruct. This can be explained by the targeting effect from the residual PBA moiety on the surface of pPBA-AND-21, because pPBA-AND-11 without residual PBA exhibited relatively less uptake. Interestingly, pPBA, by itself, showed a 6-fold and 3-fold lower uptake when compared to the 2:1 and 1:1 nanoconstructs, respectively, further indicating that the formation of a specific nanostructure with AND is another critical factor for successful cellular uptake. In addition, pre-treatment of PBA with pPBA-AND-21 reduced the internalization of nanoconstruct (2.6-fold), whereas uptake of pPBA-AND-11 was reduced 1.22-fold only, reinforcing the fact that the

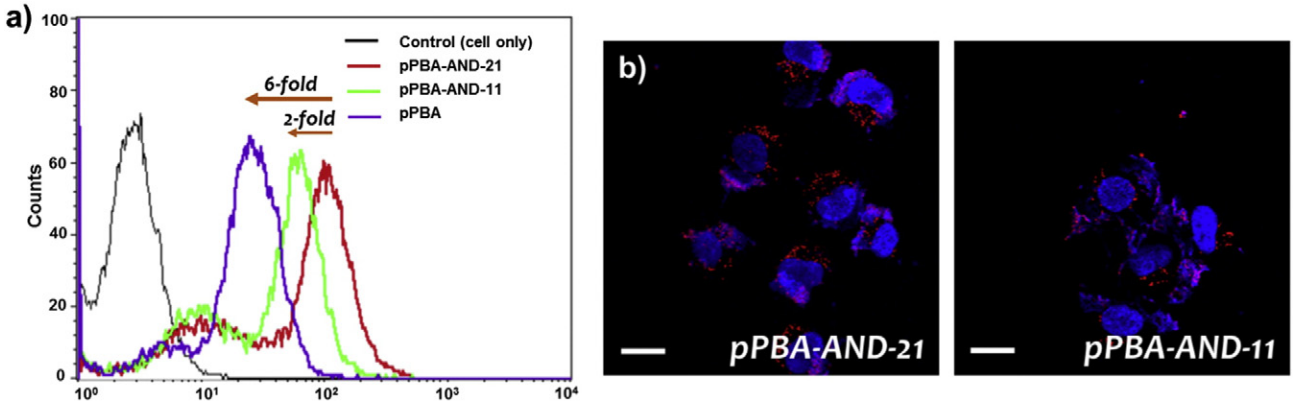

Fig. 6. Quantification of targeting effect. Cells treated with FCR-labelled pPBA-AND-11 and pPBA-AND-21 (containing 10 μM AND) were analyzed by a) flow cytometry and b) confocal microscopy.

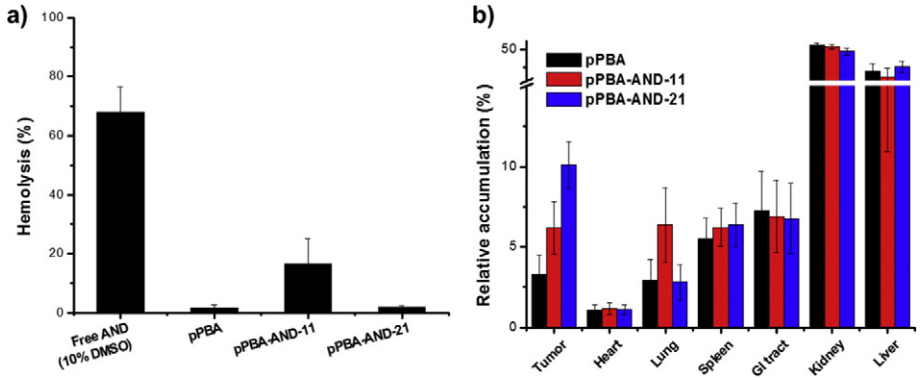

Fig. 7. Evaluation of nanoconstruct upon systemic administration. a) Hemolysis rates of pPBA, AND, pPBA-AND-11, and pPBA-AND-21. b) *In vivo* bio-distribution of pPBA, pPBA-AND-11, and pPBA-AND-21.

residual PBA on pPBA-AND-21 enhanced the targeting effect without introducing other targeting moiety (Fig. S5a–b). Moreover, the fluorescence signal of pPBA-AND-21 without free PBA was strongest than in any other formulations, in accordance with the results from flow cytometry analysis (Fig. S5c–d).

3.4. In vivo experiments using pPBA-AND nanoconstructs

In accordance with the previous results, the pPBA-AND nanoconstruct was expected to be promising at a systemic level for several reasons: 1) minimized usage of organic solvents resulting in its high water solubility and 2) absence of any positively charged molecules, which possibly leads to nonspecific toxicity. Prior to evaluating the therapeutic effect of the nanoconstruct *in vivo*, a hemolysis assay was performed at approximately the effective concentration of AND (5 mM) to ensure the blood compatibility of our pPBA-AND nanoconstructs (Fig. 7a). In the case of free AND, at least 10% of DMSO is required to solubilize the compound in an aqueous medium due to the extremely low aqueous solubility. However, it is well known that organic solvents like DMSO can induce acute hemolysis leading to drastic systemic damage. Accordingly, severe hemoglobin leakage was induced by free AND in 10% DMSO, which could cause serious anemia and crucial systemic damage. On the other hand, the high aqueous solubility of pPBA and pPBA-AND nanoconstructs enabled the formation of a nanostructure with minimal levels of organic solvent; thus pPBA, pPBA-AND-11, and pPBA-AND-21 exhibited relatively low hemolytic behavior. These results assure the safety for systemic administration of pPBA-AND nanoconstruct.

Next, the fluorescence intensity of each organ after systemic injection of samples was measured to verify the cancer-targeting ability of the PBA moiety. As demonstrated in Fig. 7b, accumulation of pPBA-AND-21 at the tumor site was 1.8-fold higher than that of pPBA-AND-11, demonstrating that the residual PBA moiety plays a pivotal role as a targeting ligand, consistent with the results obtained at a cellular level (Fig. 6a). Although the accumulation of nanoconstructs was higher at various organs like liver or kidney, cellular internalization of nanoconstructs would be lower at other organs than that of tumor due to the residual PBAs which enable specific internalization of nanoconstructs into the tumor cells. Interestingly, pPBA itself exhibited relatively lower accumulation at the tumor site compared with both pPBA-AND-11 and pPBA-AND-21. This result implies that the formation of an appropriate nanostructure is crucial for accumulation at the tumor site through the EPR effect, as previously discussed in the flow cytometry analysis.

Although the therapeutic potential of AND has emerged among various bioactive natural products, the biomedical application of AND has been hindered due to low aqueous solubility [12]. In order to challenge such drawback, a pPBA-AND nanoconstruct was formulated to introduce a tumor-targeting ability and enhance solubility. The pPBA-AND nanoconstruct exhibited great potential *in vitro*, especially for its anticancer activity, by forming a stable and water-soluble nanoconstruct. To expand the application to an *in vivo* setting, the anticancer activity of pPBA-AND nanoconstructs was evaluated against MCF-7 cancer cell xenograft mice (Fig. 8). Mice were injected with the following samples: 1) saline, 2) pPBA, 3) free AND in 10% DMSO, 4) pPBA-AND-11, and 5) pPBA-AND-21. The tumor volume was monitored every other day after systemic injection of samples. As shown in Fig. 8a, the pPBA-treated group exhibited similar tumor growth compared with that of the saline-treated group, indicating that pPBA, by itself, does not influence tumor growth. In the case of the free AND-treated group, tumor growth was inhibited to some level due to its intrinsic antitumor effect. However, as revealed by the hemolysis assay, free AND might not be suitable

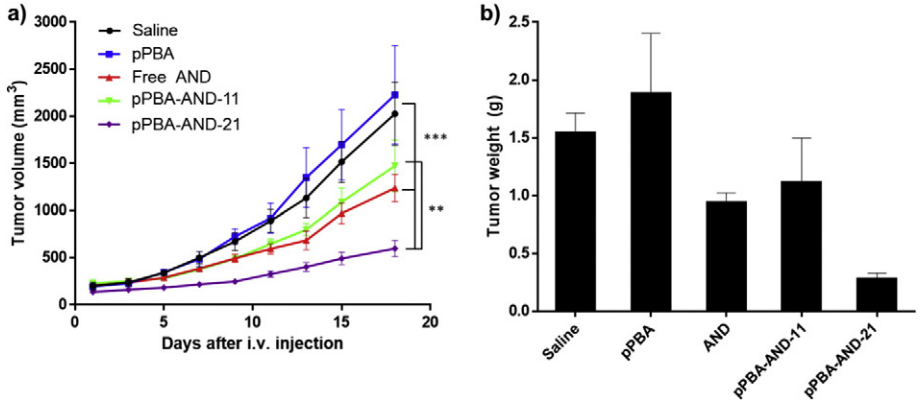

Fig. 8. *In vivo* antitumor study. a) Tumor growth profile of MCF-7 bearing balb/c nude mice after treatment with each formulation ($n = 5$; $^{**}p < 0.01$, $^{***}p < 0.001$) and b) weight of tumor at day 18.

for systemic injection because it contains an organic solvent in order to solubilize the compound. Tumor growth in the pPBA-AND-11-treated group was inhibited to a similar degree as that of free AND. Strikingly, tumor growth inhibition in the pPBA-AND-21-treated group was the highest among the samples, possibly due to several reasons: 1) high aqueous stability and blood compatibility, 2) targeting effect of residual PBA, 3) compact nano-sized structure formation, and 4) intracellular environment-specific release of AND (Fig. 8b). Body weight changes were also recorded to monitor acute toxicity, and there were no apparent body weight changes in any group, indicating that neither pPBA, AND, nor its nanoconstructs were toxic within the administered dose range (Fig. S7). These *in vivo* results definitely clarify the potential of the pPBA-AND nanoconstruct as an effective anticancer therapeutic agent by taking advantages of both PBA and AND.

4. Conclusion

In conclusion, our study demonstrated the design of a self-forming nanoconstruct based on a PBA-grafted hydrophilic polymer and AND, which is derived from a natural product, and its application for tumor-targeted and stimuli-responsive anticancer drug delivery. The binding of PBA to AND enabled the formation of a nano-sized structure in aqueous solution through a simple mixture, which permitted AND to be released in specific intracellular condition, specifically low pH and high ATP concentration. The targeting effect of the residual PBA moiety on the pPBA-AND nanoconstruct (pPBA-AND-21) was confirmed in a cellular and systemic level. Finally, our pPBA-AND nanoconstruct exhibited significant tumor growth inhibition owing to aforementioned reasons. The rationally designed nanoconstruct described herein suggests a methodological way to systemically design a delivery vehicle using boronic ester chemistry; a method that could be further applied to deliver other *cis*-diol containing drugs like doxorubicin or carbohydrate derivatives.

Acknowledgement

This research was supported by the Institute for Basic Science (IBS) in Korea (IBS-R007-G2).

Appendix A. Supplementary data

Supplementary data to this article can be found online at http://dx.doi.org/10.1016/j.jconrel.2016.10.029.

References

[1] J.T. Baker, R.P. Borris, B. Carte, G.A. Cordell, D.D. Soejarto, G.M. Cragg, M.P. Gupta, M.M. Iwu, D.R. Madulid, V.E. Tyler, Natural product drug discovery and development: new perspectives on international collaboration, J. Nat. Prod. 58 (1995) 1325–1357.
[2] M.S. Butler, The role of natural product chemistry in drug discovery, J. Nat. Prod. 67 (2004) 2141–2153.
[3] M.S. Butler, Natural products to drugs: natural product-derived compounds in clinical trials, Nat. Prod. Rep. 25 (2008) 475–516.
[4] F.E. Koehn, G.T. Carter, The evolving role of natural products in drug discovery, Nat. Rev. Drug Discov. 4 (2005) 206–220.
[5] J.W.H. Li, J.C. Vederas, Drug discovery and natural products: end of an era or an endless frontier? Science 325 (2009) 161–165.
[6] S.P. Mishra, V.G. Gaikar, Aqueous hydrotropic solution as an efficient solubilizing agent for andrographolide from *Andrographis paniculata* leaves, Sep. Sci. Technol. 41 (2006) 1115–1134.
[7] R. Wongkittipong, L. Prat, S. Damronglerd, C. Gourdon, Solid-liquid extraction of andrographolide from plants-experimental study, kinetic reaction and model, Sep. Purif. Technol. 40 (2004) 147–154.
[8] G.F. Dai, H.W. Xu, J.F. Wang, F.W. Liu, H.M. Liu, Studies on the novel α-glucosidase inhibitory activity and structure-activity relationships for andrographolide analogues, Bioorg. Med. Chem. Lett. 16 (2006) 2710–2713.
[9] T. Jayakumar, C.Y. Hsieh, J.J. Lee, J.R. Sheu, Experimental and clinical pharmacology of *Andrographis paniculata* and its major bioactive phytoconstituent andrographolide, Evid. Based Complement. Alternat. Med. 2013 (2013) 846740.
[10] J.C.W. Lim, T.K. Chan, D.S.W. Ng, S.R. Sagineedu, J. Stanslas, W.S.F. Wong, Andrographolide and its analogues: versatile bioactive molecules for combating inflammation and cancer, Clin. Exp. Pharmacol. Physiol. 39 (2012) 300–310.
[11] A. Varma, H. Padh, N. Shrivastava, Andrographolide: a new plant-derived antineoplastic entity on horizon, Evid. Based Complement. Alternat. Med. 2011 (2011) 1–9.
[12] M.L. Chen, C.Y. Xie, L.X. Liu, Solubility of andrographolide in various solvents from (288.2 to 323.2) K, J. Chem. Eng. Data 55 (2010) 5297–5298.
[13] W.J. Guo, W. Liu, G. Chen, S.C. Hong, C. Qian, N. Xie, X.L. Yang, Y. Sun, Q. Xu, Water-soluble andrographolide sulfonate exerts anti-sepsis action in mice through down-regulating p38 MAPK, STAT3 and NF-κB pathways, Int. Immunopharmacol. 14 (2012) 613–619.
[14] K. Ren, Z. Zhang, Y. Li, J. Liu, D. Zhao, Y. Zhao, T. Gong, Physicochemical characteristics and oral bioavailability of andrographolide complexed with hydroxypropyl-beta-cyclodextrin, Pharmazie 64 (2009) 515–520.
[15] K. Suresh, N.R. Goud, A. Nangia, Andrographolide: solving chemical instability and poor solubility by means of cocrystals, Chem. Asian. J. 8 (2013) 3032–3041.
[16] C. Gustafson, C. Tagesson, Influence of organic solvent mixtures on biological membranes, Brit. J. Ind. Med. 42 (1985) 591–595.
[17] A.C. Moran, M.A. Martinez, F. Sineriz, Quantification of surfactin in culture supernatants by hemolytic activity, Biotechnol. Lett. 24 (2002) 177–180.
[18] F. Mottu, M.J. Stelling, D.A. Rufenacht, E. Doelker, Comparative hemolytic activity of undiluted organic water-miscible solvents for intravenous and intra-arterial injection, PDA J. Pharm. Sci. Technol. 55 (2001) 16–23.
[19] P. Colombo, R. Bettini, P. Santi, A. DeAscentiis, N.A. Peppas, Analysis of the swelling and release mechanisms from drug delivery systems with emphasis on drug solubility and water transport, J. Control. Release 39 (1996) 231–237.
[20] L. Gao, D.R. Zhang, M.H. Chen, Drug nanocrystals for the formulation of poorly soluble drugs and its application as a potential drug delivery system, J. Nanopart. Res. 10 (2008) 845–862.
[21] R. Namgung, Y.M. Lee, J. Kim, Y. Jang, B.H. Lee, I.S. Kim, P. Sokkar, Y.M. Rhee, A.S. Hoffman, W.J. Kim, Poly-cyclodextrin and poly-paclitaxel nano-assembly for anticancer therapy, Nat. Commun. 5 (2014) 3702.
[22] B. Thierry, P. Kujawa, C. Tkaczyk, F.M. Winnik, L. Bilodeau, M. Tabrizian, Delivery platform for hydrophobic drugs: prodrug approach combined with self-assembled multilayers, J. Am. Chem. Soc. 127 (2005) 1626–1627.
[23] A. Albanese, P.S. Tang, W.C. Chan, The effect of nanoparticle size, shape, and surface chemistry on biological systems, Annu. Rev. Biomed. Eng. 14 (2012) 1–16.
[24] K.J. Cho, X. Wang, S.M. Nie, Z. Chen, D.M. Shin, Therapeutic nanoparticles for drug delivery in cancer, Clin. Cancer Res. 14 (2008) 1310–1316.
[25] W.H. De Jong, W.I. Hagens, P. Krystek, M.C. Burger, A.J. Sips, R.E. Geertsma, Particle size-dependent organ distribution of gold nanoparticles after intravenous administration, Biomaterials 29 (2008) 1912–1919.
[26] J. Kim, Y.M. Lee, Y. Kang, W.J. Kim, Tumor-homing, size-tunable clustered nanoparticles for anticancer therapeutics, ACS Nano 8 (2014) 9358–9367.
[27] G. Saravanakumar, J. Lee, J. Kim, W.J. Kim, Visible light-induced singlet oxygen-mediated intracellular disassembly of polymeric micelles co-loaded with a photosensitizer and an anticancer drug for enhanced photodynamic therapy, Chem. Commun. 51 (2015) 9995–9998.
[28] R. Haag, F. Kratz, Polymer therapeutics: concepts and applications, Angew. Chem. Int. Ed. 45 (2006) 1198–1215.
[29] J. Lee, H. Park, W.J. Kim, Nano "chocolate waffle" for near-IR responsive drug releasing system, Small 11 (2015) 5315–5323.
[30] J. Lee, C. Jeong, W.J. Kim, Facile fabrication and application of near-IR light-responsive drug release system based on gold nanorods and phase change material, J. Mater. Chem. B 2 (2014) 8338–8345.
[31] A.P. Griset, J. Walpole, R. Liu, A. Gaffey, Y.L. Colson, M.W. Grinstaff, Expansile nanoparticles: synthesis, characterization, and in vivo efficacy of an acid-responsive polymeric drug delivery system, J. Am. Chem. Soc. 131 (2009) 2469–2471.
[32] G. Cavallaro, M. Licciardi, P. Caliceti, S. Salmaso, G. Giammona, Synthesis, physicochemical and biological characterization of a paclitaxel macromolecular prodrug, Eur. J. Pharm. Biopharm. 58 (2004) 151–159.
[33] Z. Xie, H.L. Guan, X. Chen, C. Lu, L. Chen, X. Hu, Q. Shi, X. Jing, A novel polymer-paclitaxel conjugate based on amphiphilic triblock copolymer, J. Control. Release 117 (2007) 210–216.
[34] M. Dowlut, D.G. Hall, An improved class of sugar-binding boronic acids, soluble and capable of complexing glycosides in neutral water, J. Am. Chem. Soc. 128 (2006) 4226–4227.
[35] Y. Egawa, T. Seki, S. Takahashi, J. Anzai, Electrochemical and optical sugar sensors based on phenylboronic acid and its derivatives, Mater. Sci. Eng. C 31 (2011) 1257–1264.
[36] G. Springsteen, B.H. Wang, A detailed examination of boronic acid-diol complexation, Tetrahedron 58 (2002) 5291–5300.
[37] X.J. Wang, N. Xia, L. Liu, Boronic acid-based approach for separation and immobilization of glycoproteins and its application in sensing, Int. J. Mol. Sci. 14 (2013) 20890–20912.
[38] J. Yan, G. Springsteen, S. Deeter, B.H. Wang, The relationship among pK_a,pH, and binding constants in the interactions between boronic acids and diols - it is not as simple as it appears, Tetrahedron 60 (2004) 11205–11209.
[39] H.L. Liu, Y.Y. Li, K. Sun, J.B. Fan, P.C. Zhang, J.X. Meng, S.T. Wang, L. Jiang, Dual-responsive surfaces modified with phenylboronic acid-containing polymer brush to reversibly capture and release cancer cells, J. Am. Chem. Soc. 135 (2013) 7603–7609.
[40] C. Qian, Y. Chen, S. Zhu, J. Yu, L. Zhang, P. Feng, X. Tang, Q. Hu, W. Sun, Y. Lu, X. Xiao, Q.-D. Shen, Z. Gu, ATP-responsive and near-intrafed-emissive

nanocarriers for anticancer drug delivery and real-time imaging, Theranostics 6 (2016) 1053–1064.
[41] R. Mo, T. Jiang, R.D. Santo, W. Tai, Z. Gu, ATP-triggered anticancer drug delivery, Nat. Commun. 5 (2014) 3364.
[42] S. Deshayes, H. Cabral, T. Ishii, Y. Miura, S. Kobayashi, T. Yamashita, A. Matsumoto, Y. Miyahara, N. Nishiyama, K. Kataoka, Phenylboronic acid-installed polymeric micelles for targeting sialylated epitopes in solid tumors, J. Am. Chem. Soc. 135 (2013) 15501–15507.
[43] K. Djanashvili, L. Frullano, J.A. Peters, Molecular recognition of sialic acid end groups by phenylboronates, Chemistry 11 (2005) 4010–4018.
[44] A. Matsumoto, H. Cabral, N. Sato, K. Kataoka, Y. Miyahara, Assessment of tumor metastasis by the direct determination of cell-membrane sialic acid expression, Angew. Chem. Int. Ed. 49 (2010) 5494–5497.
[45] J. Kim, Y.M. Lee, H. Kim, D. Park, J. Kim, W.J. Kim, Phenylboronic acid-sugar grafted polymer architecture as a dual stimuli-responsive gene carrier for targeted anti-angiogenic tumor therapy, Biomaterials 75 (2016) 102–111.
[46] M. Ceglowski, B. Gierczyk, G. Schroeder, Poly(methyl vinyl ether-alt-maleic anhydride) functionalized with 3-aminophenylboronic acid: a new boronic acid polymer for sensing diols in neutral water, J. Appl. Polym. Sci. 131 (2014) 40778.